Chemical Science

EDGE ARTICLE

View Article Online
View Journal | View Issue

Cite this: *Chem. Sci.*, 2019, **10**, 10876

All publication charges for this article have been paid for by the Royal Society of Chemistry

Received 31st August 2019
Accepted 1st October 2019

DOI: 10.1039/c9sc04384e

rsc.li/chemical-science

Ratiometric fluorescence imaging of Golgi H_2O_2 reveals a correlation between Golgi oxidative stress and hypertension†

Hui Wang,‡ Zixu He,‡ Yuyun Yang, Jiao Zhang, Wei Zhang, Wen Zhang, Ping Li* and Bo Tang *

Golgi oxidative stress is significantly associated with the occurrence and progression of hypertension. Notably, the concentration of hydrogen peroxide (H_2O_2) is directly proportional to the degree of Golgi oxidative stress. Therefore, based on a novel Golgi-targeting phenylsulfonamide group, we developed a two-photon (TP) fluorescent probe, Np-Golgi, for *in situ* H_2O_2 ratiometric imaging in living systems. The phenylsulfonamide moiety effectively assists Np-Golgi in the precise location of Golgi apparatus. In addition, the raw material of phenylsulfonamide is easily available, and chemical modification is easily implemented. By application of Np-Golgi, we explored the generation of H_2O_2 during Golgi oxidative stress, and also successfully revealed increases on the levels of Golgi H_2O_2 in the kidneys of mice with hypertension. This work provides an ideal tool to monitor Golgi oxidative stress for the first time and novel drug targets for the future treatment of hypertension.

Introduction

Hypertension is a major risk factor for the development of cardiovascular disease (CVD).[1] It is predicted that the prevalence of hypertension will increase by more than 50% during the next 30 years.[2,3] Until now, despite receiving antihypertensive treatment, many people with the disorder still cannot adequately control their blood pressure. Thus, novel therapies are urgently needed to address resistant hypertension. A large amount of studies suggest that oxidative stress plays a central role in the pathogenesis of hypertension by perturbing the balance between reactive oxygen species (ROS) and antioxidant defenses.[4–7] Excess ROS promote hypertension by inducing endothelial dysfunction.[8,9] Therefore, complete understanding of the mechanisms of oxidative stress could contribute to the development of new therapies.

Since the Golgi complex acts as a key trafficking and sorting station and a vital biosynthetic centre for glycoproteins and lipids,[10] Golgi oxidative stress plays both physiological and pathophysiological roles in cells along with extensive ROS production.[11–13] Therefore, quantitative detection of various ROS is essential to study the mechanism of Golgi oxidative stress, especially hydrogen peroxide (H_2O_2),[14,15] an indicator of oxidative stress. However, the concentration and generation of H_2O_2 in the Golgi complex remain poorly understood to date, which is mainly due to a lack of tools for specific measurement of Golgi-located H_2O_2 *in situ*. This ultimately causes difficulties in revealing the direct relevance between H_2O_2 levels and hypertension.

Two-photon (TP) fluorescence imaging is a noninvasive approach for *in situ* detection of various biomolecules.[16–19] It exhibits increased tissue penetration depth, higher temporal resolution and less specimen photodamage than one-photon fluorescence imaging.[20] To date, many TP fluorescent probes have been developed to visualize H_2O_2 in various organelles in cells,[21–25] but *in situ* bioimaging of Golgi H_2O_2 is still scarce. Developing a TP fluorescent probe for tracing Golgi H_2O_2 in living systems could contribute to defining the relationship between hypertension and Golgi oxidative stress. However, the

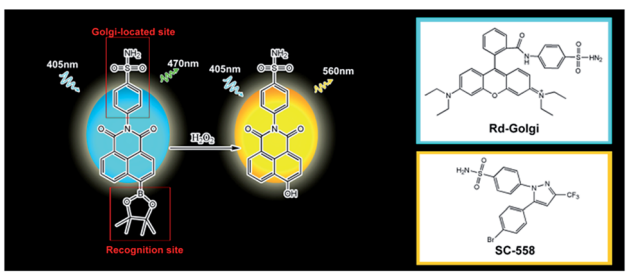

Scheme 1 The structure and response mechanism of Np-Golgi.

College of Chemistry, Chemical Engineering and Materials Science, Institute of Biomedical Sciences, Collaborative Innovation Center of Functionalized Probes for Chemical Imaging in Universities of Shandong, Key Laboratory of Molecular and Nano Probes, Ministry of Education, Shandong Normal University, Jinan 250014, PR China. E-mail: tangb@sdnu.edu.cn; lip@sdnu.edu.cn

† Electronic supplementary information (ESI) available. See DOI: 10.1039/c9sc04384e

‡ These authors contributed equally to this work.

main obstacle for the development of a TP fluorescent probe for Golgi H_2O_2 detection is a lack of precise Golgi-targeting groups. To date, two kinds of Golgi-targeting groups have been reported, including Golgi-targeting polypeptides and cysteine.[26,27] Golgi-targeting polypeptides exhibit significant localization ability but are hard to synthesize. Cysteine has limitations in the synthesis of fluorescent probes due to its low lipid solubility. Therefore, it is urgent to develop a novel Golgi-targeting group, which should meet the following requirements: (1) precise localization, (2) easily available raw material, and (3) facile chemical modification.

Previous reports have shown that the selectivity of SC-558, a Golgi protein cyclooxygenase-2 (COX-2) inhibitor, results from a phenylsulfonamide moiety that binds in specific pockets in complexes of COX-2.[28,29] Based on this work, we supposed that phenylsulfonamide could be used as a Golgi-targeting group to deliver fluorescent probes into the Golgi apparatus. We herein report the first TP ratiometric fluorescent probe, NP-Golgi, (Scheme 1) with a phenylsulfonamide moiety as the Golgi-targeting group for H_2O_2 bioimaging in the Golgi apparatus. NP-Golgi comprises phenylsulfonamide-modified 1,8-naphthalimide as a fluorescent reporter and boric acid ester as a specific H_2O_2 recognition group.[30,31] The boric acid ester converts to an electron-donating hydroxyl group upon reaction with H_2O_2, thus promoting the push–pull electron effect of the naphthalimide-conjugated system and subsequently resulting in strong fluorescence emission. In accordance with our prediction, Np-Golgi could effectively accumulate in the Golgi complex to sense H_2O_2 with high selectivity and sensitivity both *in vivo* and *in vitro*. The generation of Golgi H_2O_2 was also investigated for the first time with the assistance of Np-Golgi. With the aid of TP fluorescence microscopy, Np-Golgi was successfully applied to detect Golgi H_2O_2 fluctuations in mice with hypertension, suggesting Np-Golgi as a new instrument with which to explore the correlations between Golgi oxidative stress and diseases.

Results and discussion

Photophysical properties and selectivity of Np-Golgi

The details of the synthesis routes and characterization of Np-Golgi, and Rd-Golgi are shown in the ESI.†

We first assessed the spectroscopic properties of Np-Golgi under physiological conditions. The absorption and fluorescence spectra of Np-Golgi were measured in the absence and presence of H_2O_2. As shown in Fig. 1A, along with a colour change, a red-shift of the absorption peak of Np-Golgi from 350 nm to 446 nm occurred after reaction with H_2O_2. Meanwhile, the fluorescence emission peak was red-shifted from 470 nm to 560 nm. This demonstrated that Np-Golgi exhibited obvious changes in spectroscopic properties upon the addition of H_2O_2. We subsequently confirmed the reaction mechanism between Np-Golgi and H_2O_2 with high-performance liquid chromatography (HPLC).[32] The HPLC results showed that most Np-Golgi (HPLC retention time, TR = 50.8 min) was converted to Np-OH (TR = 25.7 min) after incubation with H_2O_2 (Fig. S1†). Meanwhile, the fluorescence quantum yield increased from

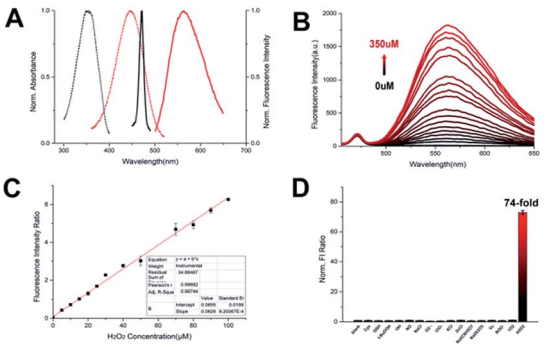

Fig. 1 (A) The absorption (dash line) and fluorescence (solid line) spectra of Np-Golgi with (red) or without (black) H_2O_2. (B) The fluorescence spectra of Np-Golgi (2 μM) with different concentration of H_2O_2. (C) Linear curve of fluorescence intensity ratio for Np-Golgi towards H_2O_2 (0–100 μM). (D) The selectivity of Np-Golgi (2 μM) in the presence of 100 μM various biologically relevant species (1–17: blank, Cys, GSH, *t*-BuOOH, ·OH, NO, NaCl, O_2^-, ClO^-, KCl, ZnCl, $Na_3C_6H_5O_7$, $Na_2S_2O_3$, Vc, ROO•, $^1O_2$, and H_2O_2).

0.30 to 0.39, and the fluorescence of the mixture (Np-Golgi and H_2O_2) was stable for at least 60 min (Fig. S2†). Then, we calculated the TP absorption cross section of Np-Golgi, which was 72 GM upon treatment with H_2O_2 (Fig. S3†).[33,34] All these results suggest that Np-Golgi potentially possesses the ability to detect H_2O_2 as a TP fluorescent probe.

We subsequently detected the fluorescence responses of Np-Golgi to various H_2O_2 levels. Upon addition of H_2O_2, the fluorescent intensity (FI) of Np-Golgi (2 μM) at 470 nm was constant, while the FI at 560 nm was significantly enhanced with higher concentrations of H_2O_2 (Fig. 1B). Notably, the F_{560}/F_{470} ratio increased 130-fold in the presence of H_2O_2 (350 μM) compared with the absence of H_2O_2. There were two linear relationships between the F_{560}/F_{470} ratio and the concentration of H_2O_2 (1–100 μM: $R^2 = 0.997$; 100–350 μM: $R^2 = 0.982$). The detection limit of Np-Golgi to H_2O_2 is 0.20 μM (Fig. 1C and S4†). These results demonstrate that Np-Golgi exhibits highly sensitive responses to H_2O_2 and can quantitatively detect H_2O_2 over a wide range.

To apply Np-Golgi to image H_2O_2 in cells and *in vivo*, we investigated the fluorescence responses of Np-Golgi to various biomolecules in cells. As shown in Fig. 1D, the FI ratio F_{560}/F_{470} of Np-Golgi was prominently increased after incubation with H_2O_2, whereas F_{560}/F_{470} was scarcely changed after incubation with other biomolecules. This result indicated that Np-Golgi exhibited remarkable selectivity for H_2O_2. We also monitored the influence of different pH values on F_{560}/F_{470}. The results showed that Np-Golgi exhibited obvious fluorescence responses to H_2O_2 at pH 6.0–8.0 (Fig. S5†). The data indicates that Np-Golgi could serve as a superior sensor for fluorescence imaging of H_2O_2 in living system.

Validation of Np-Golgi for imaging H_2O_2 in cells

To assess whether Np-Golgi could be utilized in biological systems, a standard MTT assay was performed in various cells to evaluate the cytotoxicity of Np-Golgi. The probe showed

inconspicuous cytotoxicity at concentrations less than 20 μM (Fig. S6–S8†), which demonstrated that Np-Golgi could be used in living systems. We next applied Np-Golgi for endogenous H_2O_2 detection in human hepatoma cells (SMMC7721). Phorbol 12-myristate 13-acetate (PMA, 1 μg mL^{-1}) was used to induce generation of H_2O_2 in cells. The fluorescence of Np-Golgi in the green channel (530–580 nm) increased significantly upon the addition of PMA, while the fluorescence in the blue channel (430–480 nm) was constant. The ratio of F_{green}/F_{blue} in PMA-treated cells showed 1.5-fold enhancement than in control cells. To confirm that the fluorescence enhancement was caused by increased H_2O_2 concentrations, we also evaluated the FI ratio F_{green}/F_{blue} of Np-Golgi in *N*-acetylcysteine[35] (NAC: H_2O_2 eliminator) incubated cells. As shown in Fig. S9,† both NAC-stimulated cells and PMA + NAC-stimulated cells presented negligible fluorescence in the green channel with lower F_{green}/F_{blue} ratios than control cells. This phenomenon demonstrates that intracellular H_2O_2 has been effectively eliminated. These observations validate that Np-Golgi can be used for fluorescence imaging of H_2O_2 in cells with high selectivity and good sensitivity to quantify the concentrations of H_2O_2. Next, we explored the intracellular photostability of Np-Golgi (Fig. S10†). The fluorescence of Np-Golgi was consistent for 60 min after cells were rinsed thoroughly with PBS. The result implies that Np-Golgi can be applied for long-term imaging of H_2O_2 *in vivo*.[36]

Subcellular localization of Np-Glogi

To verify the Golgi complex-targeting ability of Np-Golgi, a colocalization experiment was performed to observe the subcellular distribution of the probe. As shown in Fig. 2, the green fluorescence of Np-Golgi overlapped well with the fluorescence of the commercial probe Golgi-Tracker Red (Pearson's colocalization coefficient: 0.94) in human cervical carcinoma cells (HeLa). In the meantime, the fluorescence of Np-Golgi showed poor overlap with that of Mito-Tracker Red (0.10), Lyso-Tracker Red (0.54) and ER-Tracker Red (0.44). To further confirm that Np-Golgi possessed universal Golgi-targeting capability, colocalization experiments were also performed in SMMC7721 and human hepatic cells (HL-7702). As expected, the Np-Golgi probe also showed excellent Golgi-targeting characteristics in these cells (Fig. S11 and S12†). Collectively, Np-Golgi exhibits superior Golgi complex-locating capability in various cell types.

Subsequently, to validate that the targetability of the Np-Golgi to the Golgi complex was dependent on the phenylsulfonamide moiety, we synthesized a new phenylsulfonamide-modified fluorescent probe Rd-Golgi (Fig. S13†). Then the Golgi-targeting ability of Rd-Golgi was investigated. Rd-Golgi and Golgi-Tracker Red presented remarkable fluorescence overlap in cells with the Pearson's colocalization coefficient 0.95 (Fig. S14†). This result suggests that Rd-Golgi possesses Golgi-targeting ability and phenylsulfonamide is the crucial part of the probe for effective targeting of the Golgi apparatus. These outcomes establish that phenylsulfonamide is a powerful and universal Golgi-targeting group. In addition, compared with the reported Golgi-targeting peptide and the chemical group cysteine, phenylsulfonamide exhibits the following benefits: (1) the raw material is easily available; (2) chemical modification is simple; and (3) long-term accumulation in the Golgi is possible.

The oxidative stress of Golgi apparatus

We next applied the H_2O_2-responsive, excellently Golgi-targeting TP fluorescent probe Np-Golgi to imaging of the fluctuations in intracellular H_2O_2 associated with Golgi oxidative stress. Monensin[37,38] was used to induce Golgi oxidative stress by disturbing pH homeostasis to reduce the activity of Golgi proteins. Under NAC-pretreated conditions, monensin-stimulated cells exhibited brighter green fluorescence than NAC-incubated cells, and the F_{560}/F_{470} ratio was enhanced by

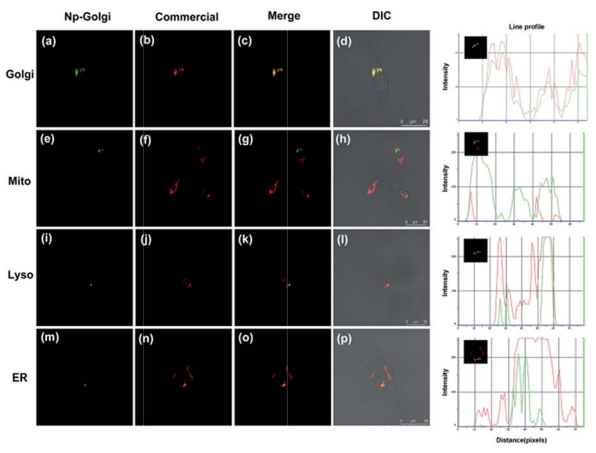

Fig. 2 Co-localization cell imaging of Np-Golgi and commercial dyes including Golgi-Red (a–d), Mito-Red (e–h), Lyso-Red (i–l), ER-Red (m–p) in HeLa cells.

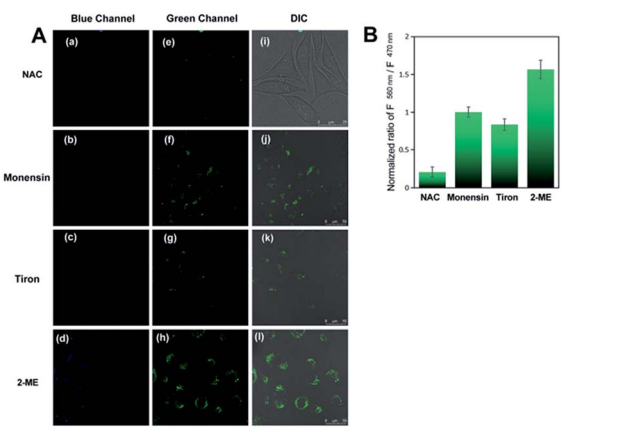

Fig. 3 (A) Fluorescence imaging of Np-Golgi after cells were treated with different stimulants. (a, e and i) NAC cells: The cells were incubated with NAC (20 mM). (b, f and j) Monensin cells: The cells were incubated with NAC and then monensin (10 μM) was added. (c, g and k) Tiron cells: the cells were incubated with NAC, and then monensin and Tiron (10 μM) were added. (d, h and l) 2-ME cells: the cells were incubated with NAC, and then monensin and 2-ME (1 μg mL^{-1}) were added. (B) Relative fluorescence intensity of Np-Golgi labelled cells from images. $n = 3$.

4.9-fold (Fig. 3A). This result shows the level of Golgi H_2O_2 is obviously increased in the Golgi oxidative stress process.

Many studies show that a large proportion of intracellular H_2O_2 is generated from superoxide anions (O_2^-) by catalysis reactions of various oxidases, such as superoxide dismutase (SOD). To seek evidence that Golgi H_2O_2 was produced from O_2^- in the Golgi oxidative stress, the fluorescence of Np-Golgi was detected after incubating cells with O_2^- inducer (2-methoxyestradiol,[39] 1.0 μg mL^{-1}) or O_2^- scavenger (Tiron,[40] 10 μM). In order to avoid the interference from cytoplasmic H_2O_2 and induce Golgi oxidative stress of the cells, NAC was used to eliminate the intracellular H_2O_2 at first, and then monensin was added to cause higher level of H_2O_2. In this case, we investigated the relations between O_2^- and H_2O_2 by using 2-ME and Tiron. As illustrated in Fig. 3, stronger green fluorescence was observed in both 2-methoxyestradiol (2-ME) and monensin co-incubated cells, and the F_{560}/F_{470} ratio was enhanced by 1.57-fold compared with monensin incubated cells. After the addition of Tiron to eliminate O_2^-, the FI of Np-Golgi in Tiron and monensin co-incubated cells decayed with a decreasing F_{560}/F_{470} ratio (by 0.83-fold) compared with monensin incubated cells. The above results indicate that the concentration of Golgi H_2O_2 has positive correlation with O_2^- levels. Collectively, these data are in excellent agreement with our prediction that Golgi H_2O_2 is mainly generated from O_2^- in Golgi oxidative stress.

TP fluorescence imaging of HBP mice *in situ*

To prove that the probe could detect H_2O_2 levels *in vivo*, we applied Np-Golgi for TP fluorescence imaging of H_2O_2 in the kidneys of mice. The animal experiments were performed in compliance with the relevant laws and guidelines issued by the Ethical Committee of Shandong University and were in agreement with the guidelines of the Institutional Animal Care and Use Committee. The probe (10 μM, 100 μL) in the LPS-injected area of the abdominal cavity of the mice showed remarkable fluorescence, and the F_{red}/F_{green} ratio was increased by 1.9-fold in the probe-injected area compared with the normal saline-injected area (Fig. S15†). This suggests that Np-Golgi could quantitatively monitor fluctuations of H_2O_2 *in vivo* through TP fluorescence imaging.

Whether high blood pressure (HBP) is accompanied by Golgi oxidative stress was further investigated. Mice were injected with either 0.9% saline (control mice) or 50 μg ouabain per day (HBP mice) for 20 days, and the blood pressure of the mice was measured three times per day. Eventually, the blood pressure of HBP mice exceeded 160 mmHg (Fig. S16†), and the results of Masson's trichrome staining of the kidneys showed that there was more collagen deposition in HBP mice than in control mice (Fig. S17†), proving that the HBP mouse model was successfully constructed. After incubation of the kidneys of mice with Np-Golgi (10 μM, 100 μL) for 30 min, the F_{red}/F_{green} ratio of the probe was compared between HBP mice and control mice combined with two-photon imaging technology. As shown in Fig. 4, the F_{red}/F_{green} ratio in HBP mice was significantly increased (by 1.8-fold) compared with that in control mice, indicating increased H_2O_2 levels in the mice with HBP. These

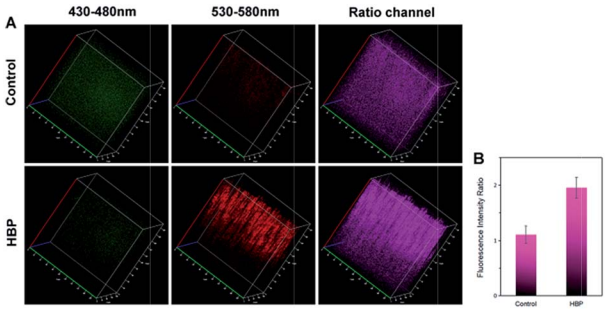

Fig. 4 TP ratiometric fluorescence imaging of kidney tissue in control mice and HBP mice with Np-Golgi. The fluorescence intensity ratio ($R_{red/green}$) of the kidneys in mice. Two-photon excited wavelength: 810 nm.

data demonstrate that pathological changes in kidney tissue in HBP mice cause severe Golgi oxidative stress and excess H_2O_2 accumulation in the process, which suggests that hypertension is closely related to Golgi oxidative stress.

Conclusion

To discover the role of Golgi oxidative stress in hypertension, we developed a novel TP ratiometric fluorescent sensor, Np-Golgi, to quantitatively detect Golgi H_2O_2 levels *in situ*. By application of Np-Golgi, we successfully detected increased levels of H_2O_2 in the kidneys of mice with hypertension. This work not only reveals the relationship between hypertension and Golgi oxidative stress, but also provides a robust tool for uncovering the connections between Golgi oxidative stress and severe diseases in the future.

Conflicts of interest

There are no conflicts to declare.

Acknowledgements

This work was supported by National Natural Science Foundation of China (21535004, 91753111, 21405097, 21390411 and 21475079), Technological Special Project for "Significant New Drugs Development" (2017ZX09301030004), the Key Research and Development Program of Shandong Province (2018YFJH0502), Natural Science Foundation of Shandong Province (ZR2017ZC0225).

Notes and references

1 S. Mendis, *Cardiovasc Diagn Ther.*, 2017, **7**, S32–S38.
2 P. M. Kearney, M. Whelton, K. Reynolds, P. Muntner, P. K. Whelton and J. He, *Lancet*, 2005, **365**, 217–223.
3 C. J. McAloon, L. M. Boylan, T. Hamborg, N. Stallard, F. Osman, P. B. Lim and S. A. Hayat, *Int. J. Cardiol.*, 2016, **224**, 256–264.
4 T. Finkel and N. J. Holbrook, *Nature*, 2000, **408**, 239–247.

5 H. Y. Small, S. Migliarino, M. Czesnikiewicz-Guzik and T. J. Guzik, *Free Radical Biol. Med.*, 2018, **125**, 104–115.
6 M. Korsager Larsen and V. V. Matchkov, *Medicina (Kaunas)*, 2016, **52**, 19–27.
7 W. Xu, Z. Zeng, J. H. Jiang, Y. T. Chang and L. Yuan, *Angew. Chem., Int. Ed.*, 2016, **55**, 13658–13699.
8 H. Matsuoka, S. Miyata, N. Okumura, T. Watanabe, K. Hashimoto, M. Nagahara, K. Kato, S. Sobue, K. Takeda, M. Ichihara, T. Iwamoto and A. Noda, *Clin. Exp. Hypertens.*, 2019, **41**, 307–311.
9 S. I. Dikalov and A. E. Dikalova, *Antioxid Redox Signal*, 2019.
10 F. Zappa, M. Failli and M. A. De Matteis, *Curr. Opin. Cell Biol.*, 2018, **50**, 102–116.
11 W. Zhong, *Clin. Exp. Hypertens.*, 2011, **3**, a005363.
12 P. Mayinger, *Clin. Exp. Hypertens.*, 2011, **3**, a005314.
13 S. W. Hicks and C. E. Machamer, *Biochim. Biophys. Acta*, 2005, **1744**, 406–414.
14 J. B. Pi, W. Qu, J. M. Reece, Y. Kumagai and M. P. Waalkes, *Exp. Cell Res.*, 2003, **290**, 234–245.
15 Q. Li, M. M. Harraz, W. Zhou, L. N. Zhang, W. Ding, Y. Zhang, T. Eggleston, C. Yeaman, B. Banfi and J. F. Engelhardt, *Mol. Cell. Biol.*, 2006, **26**, 140–154.
16 G. Masanta, C. H. Heo, C. S. Lim, S. K. Bae, B. R. Cho and H. M. Kim, *Chem. Commun.*, 2012, **48**, 3518–3520.
17 H. W. Liu, X. B. Zhang, J. Zhang, Q. Q. Wang, X. X. Hu, P. Wang and W. Tan, *Anal. Chem.*, 2015, **87**, 8896–8903.
18 E. W. Miller, A. E. Albers, A. Pralle, E. Y. Isacoff and C. J. Chang, *J. Am. Chem. Soc.*, 2005, **127**, 16652–16659.
19 W. Zhao, Y. Li, S. Yang, Y. Chen, J. Zheng, C. Liu, Z. Qing, J. Li and R. Yang, *Anal. Chem.*, 2016, **88**, 4833–4840.
20 E. J. Sanchez, L. Novotny, G. R. Holtom and X. S. Xie, *J. Phys. Chem. A*, 1997, **101**, 7019–7023.
21 B. C. Dickinson, Y. Tang, Z. Chang and C. J. Chang, *Chem. Biol.*, 2011, **18**, 943–948.
22 C. Chung, D. Srikun, C. S. Lim, C. J. Chang and B. R. Cho, *Chem. Commun.*, 2011, **47**, 9618–9620.
23 D. Kim, G. Kim, S. J. Nam, J. Yin and J. Yoon, *Sci. Rep.*, 2015, **5**, 8488.
24 J. Xu, Y. Zhang, H. Yu, X. Gao and S. Shao, *Anal. Chem.*, 2016, **88**, 1455–1461.
25 M. Ren, B. Deng, J. Y. Wang, X. Kong, Z. R. Liu, K. Zhou, L. He and W. Lin, *Biosens. Bioelectron.*, 2016, **79**, 237–243.
26 D. Srikun, A. E. Albers, C. I. Nam, A. T. Iavarone and C. J. Chang, *J. Am. Chem. Soc.*, 2010, **132**, 4455–4465.
27 R. S. Li, P. F. Gao, H. Z. Zhang, L. L. Zheng, C. M. Li, J. Wang, Y. F. Li, F. Liu, N. Li and C. Z. Huang, *Chem. Sci.*, 2017, **8**, 6829–6835.
28 R. G. Kurumbail, A. M. Stevens, J. K. Gierse, J. J. McDonald, R. A. Stegeman, J. Y. Pak, D. Gildehaus, J. M. Miyashiro, T. D. Penning, K. Seibert, P. C. Isakson and W. C. Stallings, *Nature*, 1996, **384**, 644–648.
29 H. Zhang, J. Fan, J. Wang, S. Zhang, B. Dou and X. Peng, *J. Am. Chem. Soc.*, 2013, **135**, 11663–11669.
30 M. C. Chang, A. Pralle, E. Y. Isacoff and C. J. Chang, *J. Am. Chem. Soc.*, 2004, **126**, 15392–15393.
31 A. R. Lippert, G. C. Van de Bittner and C. J. Chang, *Acc. Chem. Res.*, 2011, **44**, 793–804.
32 J. Xu, Q. Yang, X. Qian, J. Samuelsson and J. C. Janson, *J. Chromatogr. B: Anal. Technol. Biomed. Life Sci.*, 2007, **847**, 82–87.
33 Z. R. Dai, G. B. Ge, L. Feng, J. Ning, L. H. Hu, Q. Jin, D. D. Wang, X. Lv, T. Y. Dou, J. N. Cui and L. Yang, *J. Am. Chem. Soc.*, 2015, **137**, 14488–14495.
34 S. Xu, H. W. Liu, X. X. Hu, S. Y. Huan, J. Zhang, Y. C. Liu, L. Yuan, F. L. Qu, X. B. Zhang and W. Tan, *Anal. Chem.*, 2017, **89**, 7641–7648.
35 J. Xiao, J. Deng, L. Lv, Q. Kang, P. Ma, F. Yan, X. Song, B. Gao, Y. Zhang and J. Xu, *Viruses*, 2015, **7**, 2816–2833.
36 H. Y. Li, X. H. Li, W. Shi, Y. H. Xu and H. M. Ma, *Angew. Chem., Int. Ed.*, 2018, **57**, 12830–12834.
37 C. E. Machamer, *Front. Neurosci.*, 2015, **9**, 421.
38 J. I. Sbodio, B. D. Paul, C. E. Machamer and S. H. Snyder, *Cell Rep.*, 2013, **4**, 890–897.
39 P. Huang, L. Feng, E. A. Oldham, M. J. Keating and W. Plunkett, *Nature*, 2000, **407**, 390–395.
40 A. N. Ledenev, A. A. Konstantinov, E. Popova and E. K. Ruuge, *Biochem. Int.*, 1986, **13**, 391–396.